

Document downloaded from:

<http://hdl.handle.net/10251/202405>

This paper must be cited as:

Torres-Giner, S.; Chiva-Flor, A.; Feijoo, J.L. (2016). Injection-molded parts of polypropylene/multi-wall carbon nanotubes composites with an electrically conductive tridimensional network. *Polymer Composites*. 37(2):488-496.  
<https://doi.org/10.1002/pc.23204>



The final publication is available at

<https://doi.org/10.1002/pc.23204>

Copyright John Wiley & Sons

#### Additional Information

This is the peer reviewed version of the following article: Torres Giner, S., Chiva Flor, A., & Feijoo, J. L. (2016). Injection-molded parts of polypropylene/multi-wall carbon nanotubes composites with an electrically conductive tridimensional network. *Polymer Composites*, 37(2), 488-496, which has been published in final form at <https://doi.org/10.1002/pc.23204>. This article may be used for non-commercial purposes in accordance with Wiley Terms and Conditions for Self-Archiving.

# Injection-Molded Parts of Polypropylene/Multi-Wall Carbon Nanotubes Composites With an Electrically Conductive Tridimensional Network

Sergio Torres-Giner, Alberto Chiva-Flor, Jose Luis Feijoo

Specialty Plastics Division, Ferro Corporation, Carretera Valencia - Barcelona Km 61.5, 12550 Almazora, Spain

Correspondence to: S. Torres-Giner; e-mail: storresginer@hotmail.com or e-mail: Sergio.Torres@schulman.com

S. Torres-Giner is currently at A Schulman Inc., Carretera Valencia Barcelona Km 61.5, 12550 Almazora, Spain

J.L. Feijoo is currently at A Schulman Inc., Carretera Valencia - Barcelona Km 61.5, 12550 Almazora, Spain

**Abstract.** Polypropylene-based composites filled with multi-wall carbon nanotubes (MWCNTs), ranging from 1 to 6 wt%, were obtained by injection molding from a previous masterbatch compounded by twin-screw extrusion (TSE). Resultant electrical percolation phenomenon was related to the ultrathin structure of the carbonbased fillers and the high dispersion achieved in the thermoplastic matrix. In particular, conductivity experiments showed a threshold value of 3 wt% (1.3 vol%) of MWCNTs for percolation to occur. Electrical percolation was achieved as a result of the formation of an interconnected three-dimensional structure compromising a top average inter-nanotube distance of about 493 nm among isolated nanotubes in polypropylene. The current work is hoped to bear significance toward understanding of the electrical performance for industrial ultrathin carbon black-based polyolefin composites.

## INTRODUCTION

Since their discovery in 1991 by Iijima [1], carbon nanotubes (CNTs) have emerged as a new class of nanosized filler particles for use as electrically conducting components, attracting considerable interest from both academia and industry. In particular, CNTs have outstanding electrical properties, which can carry very high electric current densities of up to  $10^8$  to  $10^9$  A cm<sup>-2</sup> and can make them capable of acting as metallic-like conductors or having characteristics of a semi-conductor depending upon the distortion or “chirality” of the graphite lattice [2–4]. The graphite layer appears somewhat like a rolled-up chicken wire with a continuous unbroken hexagonal mesh and carbon molecules at the apexes of the hexagons [5, 6]. A single-walled carbon nanotube (SWCNT) is particularly formed when a single graphene sheet is wrapped into a seamless tube with a diameter of 1 nm. The chirality specifies the details of how the graphene sheet is wrapped into a SWCNT and leads to three basic classes of SWCNTs: armchair, zigzag, and chiral nanotubes [7]. A multi-walled carbon nanotube (MWCNT) is formed when SWCNTs, with increasing tube diameters, self-assemble concentrically into a single carbon nanotube. For MWCNTs with an outer diameter of 8215 nm and an inner diameter of 325 nm, density has been reported to range from 2.09 to 2.11 g cm<sup>-3</sup> [8, 9].

The outstanding electrical properties of MWCNTs can be best exploited once the nanotubes have been incorporated into some form of matrix. Use of MWCNTs as fillers in polymer composites is currently envisaged as one of the most promising area driven towards potential functional applications in electronic devices. In this regard, incorporation of very low amounts of conductive MWCNTs by conventional melt mixing techniques to an otherwise insulating polymer matrix can generate novel thermoplastic materials with certain electrical conductivity properties to, for instance, electro-static discharge and electromagnetic interference (EMI) shielding applications [10, 11]. In contrast to other conventional carbon blackbased reinforcing fillers, MWCNTs are ultrathin structures of extremely high aspect ratios that can promote transfer of its inherent properties to the polymer matrix in a much more effective manner [12–14].

The so-called percolation theory [15] is generally used to describe the insulator-to-conductor transition in composite materials consisting of conducting fillers embedded in an electrically insulating matrix. The electrical percolation threshold is particularly defined as the filler percentage in weight (wt%) or in volume (vol%) from which the electrical conductivity of a certain material increases suddenly by several orders of magnitude. When the fillers form a continuous path from one side of the matrix to the other, the composite material is above its critical filler fraction/concentration and electric current can flow through it. Nevertheless, for fewer fillers, no continuous path is formed from one side to the other and the composite material is below its critical filler fraction. Generally it is desired to have a critical filler fraction that is as low as possible, in order to have a conducting material already for a low amount of filler. A prerequisite for the latter, however, is the achievement of the spatial situation, where the randomly distributed electrically conductive fillers are able to form percolating paths in the polymer matrix. For this, as expected, selection of the polymer and the method of incorporation of the filler is decisive. Shaffer and Windle [16] reported that poly(vinyl alcohol)/CNTs composites associate a percolation threshold between 5 and 10 wt%.

However composites based on epoxy resins, as described by Sandler et al. [17], produced by curing of nanotube dispersions in the liquid precursor for polymerization, were found to exhibit a percolation threshold as low as 0.04 wt%. These huge changes in percolation threshold have been attributed to the polymer layer adsorbed around the nanotubes that reduces the quality and quantity of electrical contacts among CNTs. It is worth stressing that, though incorporation of CNTs are known to modify the crystallization behavior of semi-crystalline polymers under certain processing conditions, variances in conductivity do not actually originate from the amorphous or crystalline nature of the polymer matrix. As a matter of fact, previous research work carried out by Grossiord et al. [18] reported that the formation of crystallites in a commercial maleic anhydride-grafted isotactic polypropylene system, with particular crystal growth direction perpendicular to the individual nanotubes, did not disrupt the electrically conductive network. This was also in full agreement with earlier data on SWCNT/polyethylene nanocomposites, which displayed similar conductivity levels despite a substantially dissimilar degree of crystallinity (33% vs. 78%) [19]. This unambiguously evidences that there is no preferential accumulation of CNTs in the amorphous phase, which would affect the percolation threshold of semi-crystalline polymers.

Furthermore, the achievement of electrical conductivity does not only depend on the nature of the nanotube–polymer interface, but it can be also considered as a “geometrical issue” depending on CNT length, orientation, and particularly dispersion state. Owing to the tendency of nanotubes to remain bundled or highly entangled, caused primarily by van der Waals attracting forces, the challenge on preparing CNT-based polymer composites by melt compounding lie in uniformly dispersing the nanotubes. For this, the polymer chains have to necessarily infiltrate during processing into the primary agglomerates [20]. In this respect, it is worth noting that the preparation of a masterbatch, i.e. a concentrate containing high amounts of highly pre-dispersed CNTs in a miscible polymer resin with additional synergistic additives, provides a very simple preparation method for subsequent incorporation into commercial thermoplastic materials by conventional melt compounding and shaping methods. However, in our literature survey, homogeneous dispersion of pristine MWCNTs in a polymer masterbatch has scarcely been reported up to now.

Twin-screw extrusion (TSE) delivers more mixing and dispersion energy than that provided by conventional single-screw extruders. TSE has superior heat and mass transfer capabilities and offer greater control over residence time distribution (RTD) [21]. In particular, corotating intermeshing twin-screw extruders lead to high dispersive mixing in terms of melt homogenization and solids breakup, making them particularly attractive to prepare polymer nanocomposites. The two-lobe design of the screw is

virtually the standard. Screws are particularly made up of conveying elements, kneading blocks, and mixing sections. The polymer is positively transferred from one screw channel to the other screw channel in the intermeshing region by the wiping action of the intermeshing flight. The polymer melt makes a “figure-8” path going through both screws [22]. Kneading blocks involve several discs staggered at an angle to one another, ranging habitually from 30 to 90, the motion of which causes intense shearing and has a chopping effect on the melt stream. Gear teeth are habitually arranged to form a helix in the mixing sections of the screws to provide excellent distributive mixing without high dispersive stresses. Although gear mixers are typically used for mixing liquid additives with molten polymers, they have been tried with glass fibers and other applications [23].

During TSE compounding, while polymer resins are fed through main feed hoppers, CNTs are preferably fed downstream through a side feeding port. This is done in order to increase pronounced intercalation into the polymer matrix, reduce the risk of nanotubes deterioration during processing, and to control the thermal history. In relation to other processing conditions, the uses of low melt viscosity systems have demonstrated to significantly support to reduce the average inter-fillers distance for both CNTs and carbon black polymer composites [24–26]. In the latter studies, it was indeed shown that either increasing the processing temperature [24] or reducing the molecular weight of the polymer matrix [26], hence decreasing the melt viscosity, lowers the percolation threshold of the resultant composites. It can be therefore suggested that low viscosities and short residence times can result helpful in achieving optimum dispersion of CNTs.

Injection molding certainly represents a cost effective melt processing methodology to produce a large number of plastic parts, including polymer/CNTs composites [27]. In this process, polymer resins are fed into the rear part of the injection screw in pelletized form while MWCNTs can be incorporated in powder or, much preferably, by means of a masterbatch. Once the polymer is melted (semi-crystalline polymers) or plasticized (amorphous polymers) by the rotating screw (called a reciprocating screw) against the unmoving barrel wall, a metered dosage of polymer melt is then transferred towards the nozzle of the injection unit and injected into the mold, where the heat from the melt dissipates rapidly into the mold. When the part is rigid enough, then it is ejected from the mold and the cycle repeats. In general very high shear rates arise in injection molding operations, usually up to  $10^4 \text{ s}^{-1}$ . To limit temperature increases from viscous heating and also to facilitate easy filling, polymer grades of low viscosity, i.e. resins with high melt flow index, are habitually selected.

The injection process conditions can strongly influence on the electrical conductivity of the molded parts of CNT-based composites by inducing considerable shear stress and heat to the composite melt [28]. Mold cavity filling is characterized by the “fountain effect,” in which elements of the molten

polymeric fluid undergo complex shear and stretching motions as they catch up the free flow front and then move outwards to the cold walls [21]. This phenomenon can impart considerable orientation to the resulting injection molded parts. While molecular orientation is consistently appointed in extrusion to improve the mechanical properties, in injection molding orientation generally represents a nuisance [29]. A good strategy to elude such orientation is reducing high shear rates. Alternatively, rapid solidification on the mold walls should be also restricted in order to avoid the formation of the so-called “skin-core” structure, i.e. a heterogeneous distribution of oriented versus non-oriented polymer crystallization morphology in which the surface generally has a higher electrical resistivity than the core [30]. Reducing the injection speed and increasing the melt temperature, which increases the mobility of the polymer chains, can be utilized as an effective tool to reduce the degree of orientation and rebuilding of the nanotubes network. In general, a partially aligned structure of CNTs is preferred to obtain highest electrical conductivity values [31].

As previously anticipated, in addition to the polymer matrix and the preparation process, the electrical percolation threshold of a given composite is reasonably dependent on the intrinsic properties of the fillers. Shapes and sizes of CNTs play an important role in determining the percolation threshold of the polymer composite. In particular, aspect ratio, i.e. length to width relation, is thought to play a large role in percolation threshold as it appears that conductive percolation paths are, in general, more easily set up when homogeneous dispersion of long and thin nanotubes is achieved. Several research studies have demonstrated that aspect ratio of MWCNTs is the main parameter in determining the conductive properties of polymer composites [32–34]. This has been fully supported by other studies, in which it was concluded that an increase in the aspect ratio of CNTs consistently implies an exponential decrease in percolation threshold of the composite [35, 36]. The work of Natsuki et al. acutely investigated the relation between percolation behavior and orientation as well as the aspect ratio of the fillers [37].

The preparation of polypropylene/MWCNTs composites using injection molding via masterbatch is described herein and the analysis of the conducting properties are evaluated and discussed according to the morphological characteristics. The percolation threshold in electrical conductivity of the polymer composites was determined by varying the MWCNT content, while keeping the processing conditions constant. This study sheds some light on the relation of the electrical conductivity phenomenon to the formation of the electrically conductive network.

## EXPERIMENTAL SECTION

### Materials

MWCNTs grade NC7000 from Nanocyl™ (Sambreville, Belgium) were used as received without further purification. Commercial polypropylene homopolymer ISPLEN<sub>VR</sub> PP-070 G2M from Repsol (Madrid, Spain) with a melt flow index of 12 g/10 min (230C, 2.16 kg), density  $\rho = 0.91 \text{ g cm}^{-3}$ , and volume resistivity  $R_{510} = 10^{13} \text{ X cm}^{-1}$  was employed for the injection molding process.

### Twin-Screw Extrusion

Preparation of a proprietary polypropylene-based masterbatch containing 20 wt% of MWCNTs was carried out at Ferro’s facilities (Almazora, Spain) using a W&P ZSK25 intermeshing co-rotating twin-screw extruder, followed by water bath cooling and pelletization. The screw profile and operation conditions (barrel temperature 190C, screw speed 400 rpm, output:  $18 \text{ kg h}^{-1}$ ) were chosen in order to maximize filler dispersion.

### Injection Molding

Dried pellets of the previously obtained masterbatch were diluted into the injection-grade polypropylene in the main feed hopper at the following weight contents: 1, 2, 3, 4, 5, and 6 wt%. This was carried out using an Arburg AllRounder 305-210-700 model at an injection speed of  $20 \text{ mm s}^{-1}$  and a melt temperature of 225C. Composite pieces with a size of  $13 \times 5 \times 6 \times 3 \times 12.5 \text{ mm}^2$  and thickness (m) of 4 mm were obtained.

### Thermal Stability Measurement

Thermogravimetric analysis using a Mettler–Toledo TGA/SDTA 851e model was conducted to identify the thermal stability of MWCNTs. TGA curves were obtained on 10-mg sample under air atmosphere (ca. 79%  $\text{N}_2$ , 21%

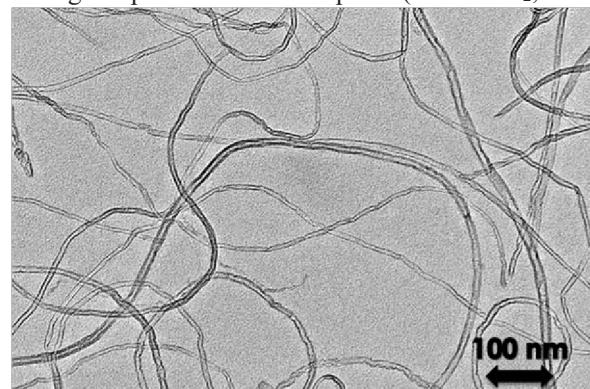


FIG. 1. TEM micrograph, at 325,000, of MWCNTs. Scale marker of 100 nm.

O<sub>2</sub>) at a heating rate of 10C min<sup>-1</sup> from room temperature to 800C.

### Morphology

Transmission electron microscope (TEM) was performed on the MWCNT powder by means of a Jeol JEM2100F microscope with an accelerating voltage of 200 kV. Scanning electron microscope (SEM) was carried out on the polymer composites using a JEOL 7001F microscope with an accelerating voltage of 15 kV. For this, the injection molded pieces were initially cryofractured in liquid nitrogen, and then glued to a copper plate using silver. Composite morphology information was finally obtained from cross-sectional fractures of the pieces.

Schematic representation of the nanotubes network formed in the composite pieces was obtained by processing the resultant SEM images with Autocad 2010 software. Fictional lines were used to simulate connections among adjacent nanotubes. A maximum distance of 1 mm was fixed for all measurements. The average distance for each composite was determined manually by means of the Autocad software measuring tool from the SEM micrographs in their original magnification.

### Conductivity Measurements

Conventional two-point-probe method was employed to measure the direct current (DC) electrical resistivity (R) of the composites pieces at room temperature [38]. Conductive silver paint was applied on both sides of the injection molded parts to ensure good contact of the sample surface with the electrodes. Minimum of five tests were performed for each specimen, along the 3 directions, and the data were averaged. The volumetric conductivity ( $\sigma$ ) was given by the following equation:

$$\sigma = \frac{L}{R \cdot A} \quad (1)$$

The conductivity of the injection molded parts was further rationalized in terms of the modified classical percolation theory:

$$\sigma = \sigma_0 (\frac{u}{u_c} - 1)^t \quad (2)$$

where  $u$  is the volume fraction of the filler,  $u_c$  is the volume percolation concentration,  $\sigma_0$  is the conductivity of the filler, and  $t$  is the critical exponent. For a single percolation system, the critical exponent reflects the dimensionality of the composites and follows a power-law dependence of 2 (1.6–2) in a three dimensional, and 1–1.3 in a two-dimensional system [39].

## RESULTS AND DISCUSSION

### Polymer Composites

The transmission electron microscopy (TEM) image of the pristine MWCNTs, presented in Fig. 1, indicates direct evidence for the existence of hollow fiber-like structures. In particular, the carbon-based fillers presented a relatively high length  $L$  (122  $\mu$ m) and a very low diameter  $D$  (ca. 10 nm). Average aspect ratio, defined as the  $L/D$  fraction, was determined to be about 150.

The TGA analysis of the MWCNTs was conducted to ascertain their thermal stability in air atmosphere, which certainly represents a more oxidative condition than that found during the extrusion process. The relative mass loss due to the oxidation of the carbon material and the first derivative curve are shown in Fig. 2. This directly reflects the variation in weight as a function of temperature by occurrence of thermal events. It can be seen that no significant mass loss occurs below 490C and the maximum mass loss was occurred at about 650C. This indicates that the sample contains a negligible amount of carbonaceous impurities. Once temperature exceeds the degradation onset temperature, the thermal decomposition of the strong CAC bonds of the nanotubes takes place. In addition, the residual catalyst content at 800C is extremely low, below 0.3 wt%. These results are in accordance with other previous studies on the thermal stability of MWCNTs in their pristine form [18] and [40].

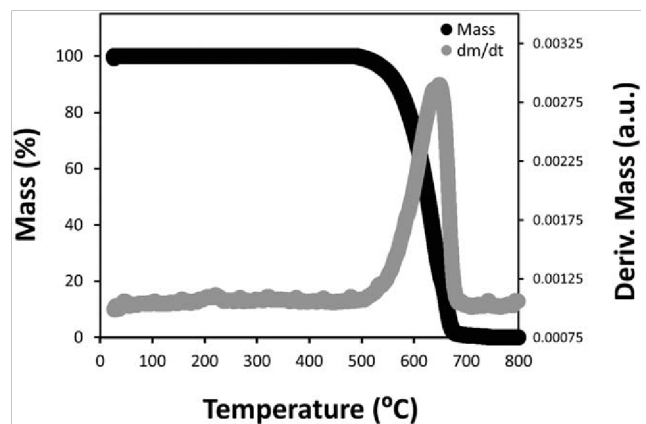


FIG. 2. Thermogravimetric curves from room temperature to 800C showing thermal stability of MWCNTs in air atmosphere.

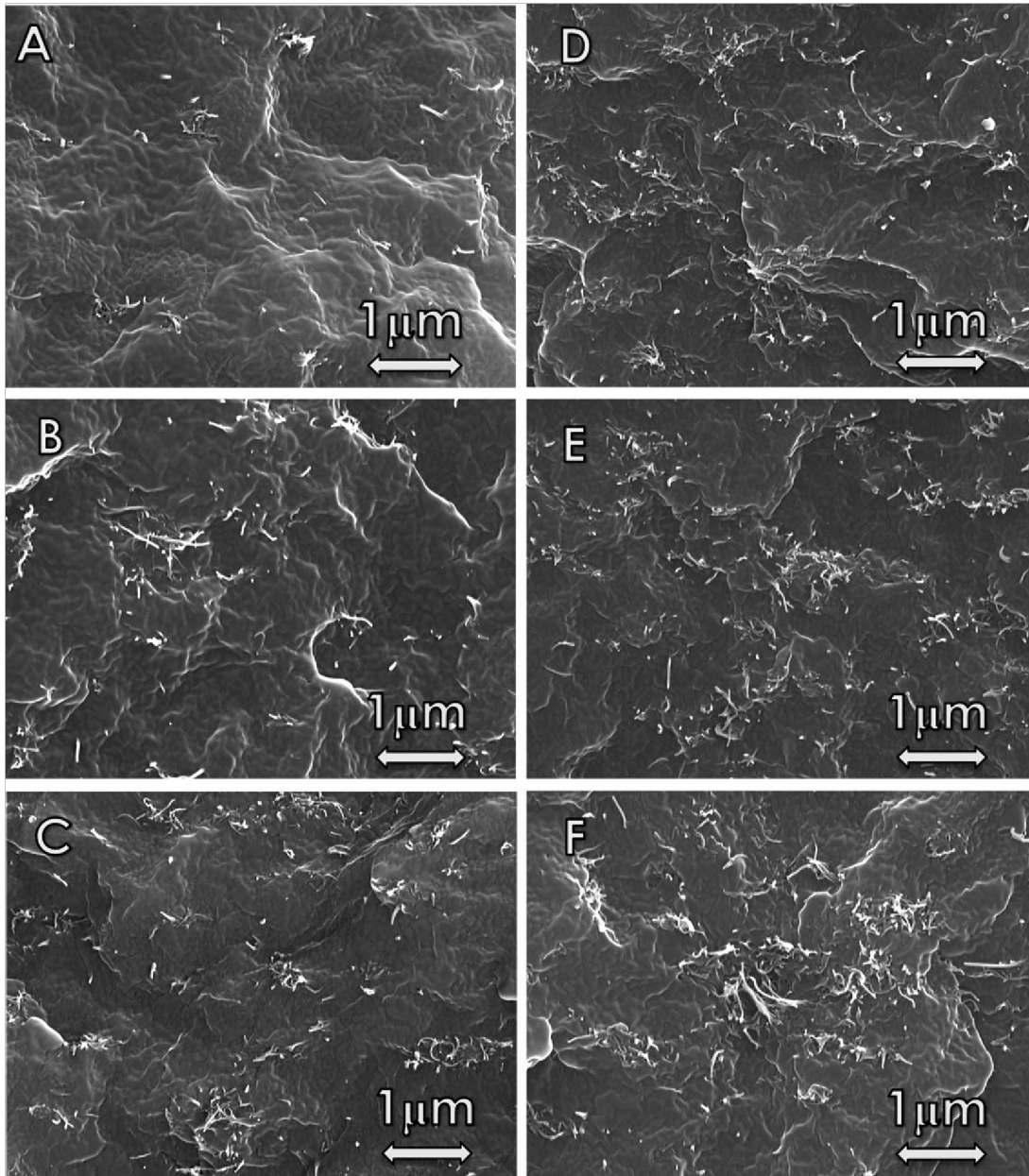


FIG. 3. SEM micrographs, at 315,000, of the fractured surface in the length direction of the polypropylene composites containing: (A) 1 wt% of WMCNTs; (B) 2 wt% of WMCNTs; (C) 3 wt% of WMCNTs. (D) 4 wt% of WMCNTs; (E) 5 wt% of WMCNTs; (F) 6 wt% of WMCNTs. Scale markers of 1  $\mu\text{m}$  in all cases.

Morphological studies were carried out on the polymer composites in order to investigate the degree of dispersion of the MWCNTs in the injection molded parts. Figure 3 provides insight into the composite structures for the nanotubes distribution in the polypropylene matrix. As it can be observed, when the content was 1 wt% (Fig. 3A), MWCNTs were seen to be incorporated mainly as isolated dispersed fibers presenting very small bundled agglomerations in the polymer matrix. Individual MWCNTs were also prevalent in Fig. 3B, where no large bundles were discernible. The presence of isolated nanotubes would indicate a high degree of dispersion but also that these filler loadings could not be sufficient yet to provide an interconnected structure. When the amount of MWCNTs

was increased to 3 wt% (Fig. 3C), a slight formation of dispersed array of nanotubes in the polypropylene matrix was observed. When the concentration was further increased to 4 wt%, in Fig. 3D, the MWCNT network became obviously denser and the presence of nanotubes groups also increased. At 5 wt%, the network of nanotubes became much more established (Fig. 3E). Thereafter, the density of the network obviously increased and the MWCNTs became much more agglomerated (Fig. 3F). In general, the distribution of MWCNTs in the polypropylene matrix was relatively uniform even at high filler concentrations.

To achieve electrical conductivity, CNTs ideally have to be physically contacted with one another and electron must overcome contact resistance [15, 41]. However, when direct

contacts are not available, electric current would flow by means of tunneling or jumping, in which electron must overcome a barrier potential that is related to the distance between the adjacent CNTs and the electrical resistivity of the polymer matrix [42, 43]. Figure 4 represents the schematic pathways or projected electric flows among nanotubes in the polypropylene matrix as a function of the filler concentration. As it can be seen in the figure, at low filler contents, i.e. in the range 1–2 wt%, the network is poorly connected which does not allow the formation of conducting channels. However, as expected, the increase in MWCNTs loading intensified the presence of conductive sites in the composites as it reduced the nanotube-nanotube distances. In this sense, from 3 to 4 wt%, a more number of conductive networks can be observed in the composites to facilitate the electron hopping phenomenon and, as a result of this, to decrease the electrical resistivity. At higher loadings, i.e. 5 and 6 wt%, the network of nanotubes became firmly established.

Figure 5 displays the distribution of distances among adjacent MWCNTs for each composite, which were obtained from previously schematic representations. Low composite contents show a sharp bimodal distribution of inter-nanotube distances: about 69 and 610 nm for 1 wt%, and about 76 and 585 nm for 2 wt%. This would indicate that MWCNTs were mainly distributed as isolated as well as grouped nanotubes, fact that was previously observed in the morphological analysis. For 3 and 4 wt% contents, composites still retained the bimodal distribution but average distances among isolated nanotubes (second peak) was seen to decrease considerably. In particular, this was reduced to about 493 and 367 nm for 3 and 4 wt% of MWCNTs, respectively. At high filler contents, the composites presented a monomodal distribution and the inter-nanotube distance was determined at about 226 and 131 nm for 5 and 6 wt%, respectively. Present result would point out that, for high loaded composites, nanotubes were predominantly agglomerated and distributed along the whole polypropylene matrix, which supports the fact that the MWCNTs were properly interconnected.

### Electrical Conductivity

In light of the well-dispersed MWCNTs, composites are expected to present electrical conductivity due to formed networks of conducting nanotubes throughout the insulating polypropylene matrix. Electrical conductivity ( $\sigma$ ) as a function of weight (wt%) and volume percent (vol%) of MWCNTs is displayed in Figure 6. Electrical conductivity can be observed to remain nearby the electrostatic range ( $10^{29}$  S cm<sup>-1</sup>) below 2 wt% of filler content. Conductivity increases monotonously with growing content of MWCNTs in the composite from 3 to 4 wt%. At this range of filler concentration, the electrical conductivity particularly

increased by six orders of magnitude, from  $10^{28}$  to  $10^{22}$  S cm<sup>-1</sup>. This sharp change in the material resistivity can be regarded as the electrical percolation threshold. Above this, for higher filler concentrations, i.e. 5 and 6 wt%, the electrical conductivity is seen to increase marginally with increasing MWCNTs content.

As can be also seen in Figure 6, composites with highest loadings of MWCNTs possessed a conductivity of  $10^{21}$  S cm<sup>-1</sup>. In addition, injection molded pieces generated a relatively low percolation threshold of 1.3 vol%. Present values, to the best of our knowledge, represent high electrical conductivities for MWCNTs in polypropylene obtained by a non-solution mixing method in general, and using conventional melt processing technology in particular. These are, for instance, in accordance with values given by Hagerstrom and Greene [44], who found a volume resistivity of  $10^2$  Ohm cm<sup>-1</sup> for 5 wt% of MWCNTs in polycarbonate. However, as a polymer with polar groups and aromatic structures, polycarbonate is expected to present lower interfacial energy with unmodified MWCNTs than polypropylene. Furthermore, the threshold attained here is about 3 times lower than the 9–18 wt% range reported by Lozano et al. [45] in polypropylene for vapor grown carbon nanofibers prepared using Haake miniature laboratory melt mixer. The current threshold is also moderately smaller than those reported by Ngabonziza et al. [46] and King et al. [47] who obtained a percolation threshold in polypropylene by injection molding of 3.8 wt% and 2.1 vol%, respectively. In fact, previous studies proved that electrical conductivities of MWCNT/polypropylene composites prepared by melt mixing techniques were relatively difficult to achieve due to the disruption of MWCNT connections during processing [48].

The resultant high electrical resistivity can be understood in terms of the short inter-nanotube distance required for the electron flowing, as previously depicted in Fig. 4 and numbered in Fig. 5. At the percolation threshold, the distance among isolated nanotubes was previously estimated to be reduced from about 493 to 367 nm (from 3 to 4 wt% of MWCNTs). Below this distance, it is suggested that electrons can tunnel or hop among nanotubes at the junctions of the percolation network. This reduction of the average inter-nanotube distance results critical in the conductive properties because it essentially promotes the formation of conductive pathways inside the polypropylene matrix and therefore the conversion of the polypropylene polymer from an insulator to a semi-conductor material. This can be mainly attributed to the large aspect ratio of MWCNTs and the relatively high degree of dispersion accomplished during the masterbatch compounding by TSE and subsequent injection molding process, which are supported by the previously mentioned morphological results.

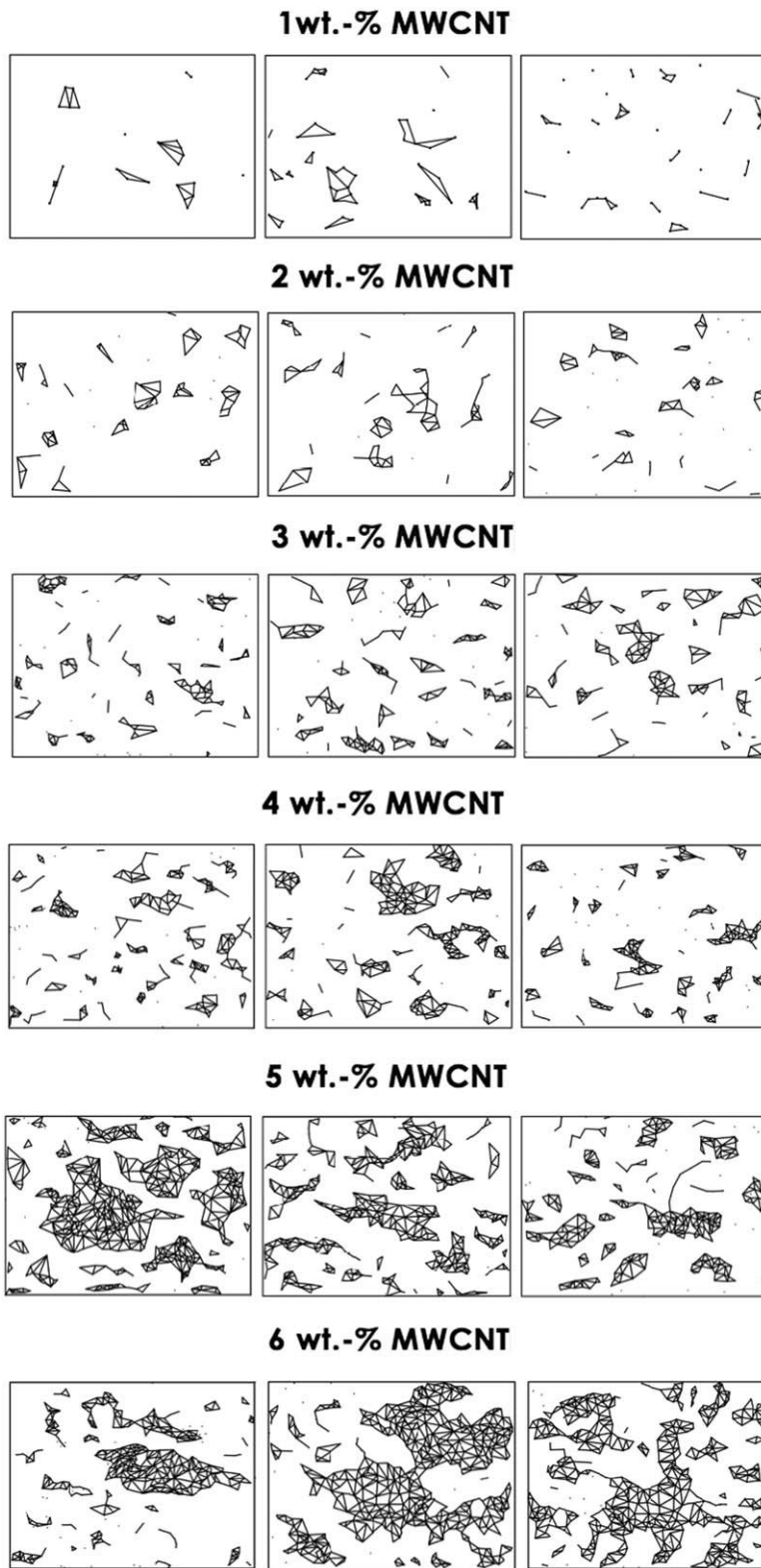


FIG. 4. Schematic representation of the electrical conductive pathway of the MWCNTs in the polypropylene composites containing, from top to bottom, 1 wt% of WMCNTs, 2 wt% of WMCNTs, 3 wt% of WMCNTs, 4 wt% of WMCNTs, 5 wt% of WMCNTs, and 6 wt% of WMCNTs.



Finally, from data in Figure 7,  $t$  was estimated to be firms that the MWCNTs were located on the whole vol1.82, which reveals the presence of an interconnected ume of the polypropylene matrix, resulting in a relatively three-dimensional conductive structure. This result con- well dispersed network of nanotubes.

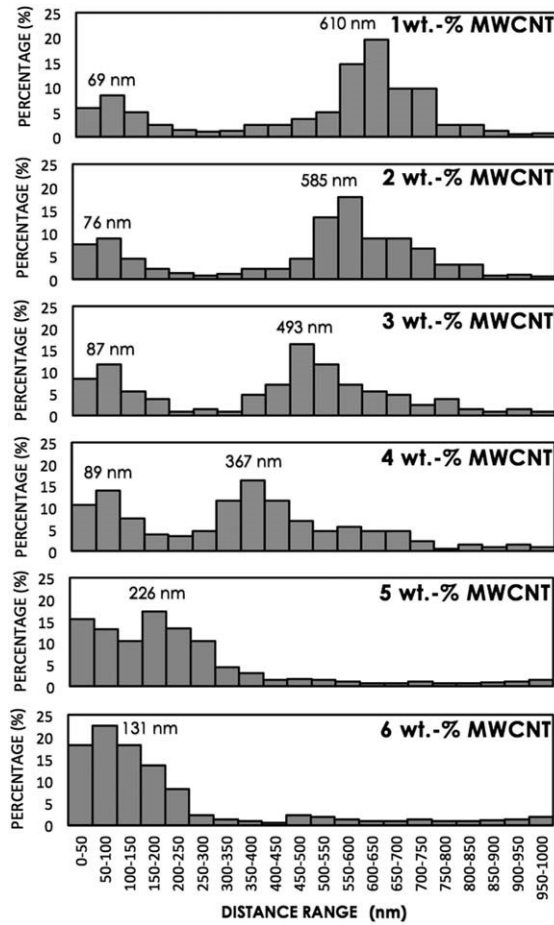


FIG. 5. Distance distribution among adjacent nanotubes in the polypropylene composites containing, from top to bottom, 1 wt% of WMCNTs, 2 wt% of WMCNTs, 3 wt% of WMCNTs, 4 wt% of WMCNTs, 5 wt% of WMCNTs, and 6 wt% of WMCNTs.

## CONCLUSIONS

Electrical conductivity of MWCNT-filled polypropylene composites prepared from a masterbatch compounded by TSE and subsequent injection molding was investigated depending on the polymer composite morphology and

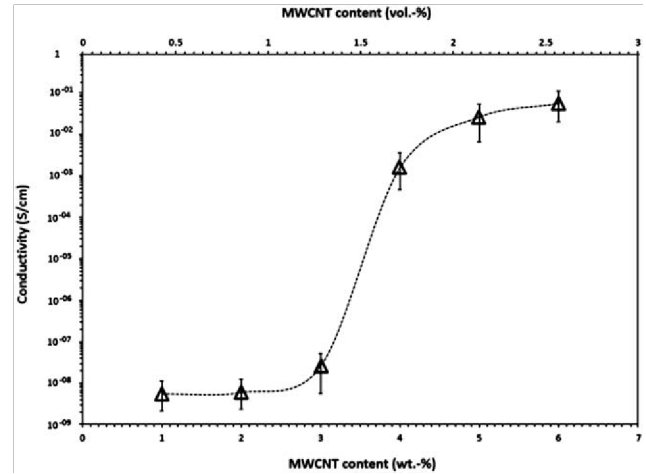


FIG. 6. Electrical conductivity as a function of the MWCNT content for the injection molded polypropylene composites.

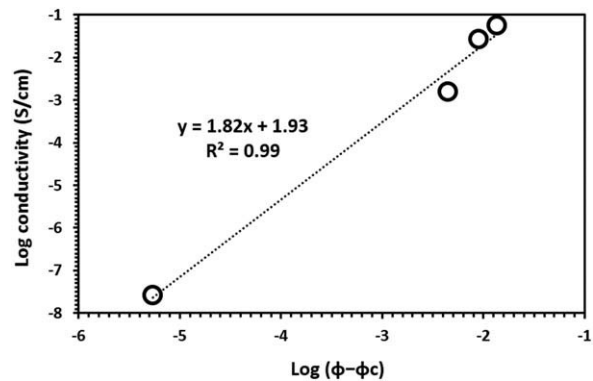


FIG. 7. Log-log plot of the conductivity versus  $u_{2u_c}$ .

related to a critical inter-nanotube distance. A low electrical resistivity was achieved by thoroughly dispersing the MWCNTs in the polypropylene to form a polymer composite with an interconnecting three-dimensional structure of nanotubes. Obtained conductive polypropylene composites needed very low filler loadings, about 4 wt% to achieve electrostatic dissipation, compared to about 10–20 wt% for typical technical carbon black-based compounds [49].

This has been widely accepted that a conductive network is essentially produced by the establishment of uninterrupted clusters of connected conducting fillers. Interestingly, present research work also revealed that the presence of neighboring conductive sites can facilitate the hopping or jumping of electron when direct contacts are not completely available. In particular, this demonstrates that when distance among adjacent isolated nanotubes is reduced below a critical value, in the case of polypropylene it was about 493

nm, it provides the formation of the necessary conductive channels for electric charge to flow. Present results could be extrapolated to other systems including SWCNTs and other polymer materials.

Major commercial application of MWCWNT-based composites can found their use as electric conducting components and devices. Resultant injection molded pieces can pave the way for potential new applications in materials requiring low electrical resistivity such as high performance electrostatic dissipative plastics or coatings. For electrostatic dissipation, for example, the conductivity level should be in the range between  $10^{28}$  and  $10^{23}$  S m<sup>-1</sup>. On the other hand, for EMI shielding applications, an electrical conductivity in excess of 1 S m<sup>-1</sup> should be targeted. When the conductivity is above  $10^{23}$  S m<sup>-1</sup>, the materials are considered (semi-)conductive [50]. These conductive properties embedded in a low density plastic such as polypropylene definitely give a new alternative for higher density metallic parts or costly metal coated parts. Additionally the low loading levels and the ultrathin morphology of the MWCNTs would allow electrical conductivity to be achieved while avoiding or minimizing impairment of other performance aspects, such as mechanical properties and processing viscosity, which can be very low in for instance thin-wall molding applications.

#### ACKNOWLEDGMENTS

The Career and Employment Office of the UPV is acknowledged for the collaboration through the Educational Cooperation Programs. Thanks are also due to Bego~na Galindo from AIMPLAS (Paterna, Spain) for supplying raw materials and to UJI-SCIC for the support during the morphological characterization on the composites pieces.

#### REFERENCES

1. S. Iijima, *Nature*, 354, 56 (1991).
2. A.B. Dalton, S. Collins, E. Munoz, J.M. Razal, V.H. Ebron, J.P. Ferraris, J.N. Coleman, B.G. Kim, and R.H. Baughman, *Nature*, 423, 703 (2003).
3. S. Frank, P. Poncharal, Z.L. Wang, and W.A. de Heer, *Nature*, 280, 1744 (1998).
4. M.F. Yu, O. Lourie, M.J. Dyer, K. Moloni, T.F. Kelly, and R.S. Ruoff, *Science*, 287, 637 (2000).
5. J.W.G. Wildoer, L.C. Venema, A.G. Rinzler, R.E. Smalley, and C. Dekker, *Nature*, 391, 59 (1998).
6. T.W. Odom, J.L. Huang, P. Kim, and C. Lieber, *Nature*, 391, 62 (1998).
7. M. Terrones, *Annu. Rev. Mater. Res.*, 33, 419 (2003).
8. Q. Huang, L. Gao, Y. Liu, and J. Sun, *J. Mater. Chem.* 15, 1995 (2005).
9. Q. Lu, G. Keskar, R. Ciocan, R. Rao, R.B. Mathur, A.M. Rao, and L.L. Larcom, *J. Mater. Chem.*, 110, 24371 (2006).
10. E.T. Thostenson, Z.F. Ren, and T.W. Chou, *Comp. Sci. Tech.*, 61, 1899 (2001).
11. M.T. Byrne and Y.K. Gun'ko, *Adv. Matter.*, 22, 1672 (2010).
12. D. Qian, E.C. Dickey, R. Andrews, and T. Rantell, *Appl. Phys. Lett.*, 76, 2868 (2000).
13. L. Jin, C. Bower, and O. Zhou, *Appl. Phys. Lett.*, 73, 1197 (1998).
14. Y. Wang, J. Wu, and F. Wei, *Carbon*, 41, 2939 (2003).
15. S. Kirkpatrick, *Rev. Mod. Phys.*, 45, 574 (1973).
16. M.S.P. Shaffer and A.H. Windle, *Adv. Mater.*, 11, 937 (1999).
17. J. Sandler, M.S.P. Shaffer, T. Prasse, W. Bauhofer, K. Schulte, and A.H. Windle, *Polymer*, 40, 5967 (1999).
18. N. Grossiord, M.E.L. Wouters, H.E. Miltner, K. Lu, J. Loos, B. Van Mele, and C.E. Koning, *Eur. Polym. J.*, 46, 1833 (2010).
19. R. Haggemueller, C. Guthy, J.R. Lukes, J.E. Fischer, and K.I. Winey, *Macromolecules*, 40, 2417 (2007).
20. P.J.F. Harris, *Carbon Nanotube Science: Synthesis, Properties and Applications*, Cambridge University Press, Cambridge, UK (2009).
21. J. Vlachopoulos and D. Strutt, *Mater. Sci. Tech.*, 19, 1161 (2003).
22. C.I. Chung, *Extrusion of Polymers: Theory and Practice*, Hanser, Munich (2000).
23. H.F. Giles, J.R. Wagner Jr., E.M. Mount III, *Extrusion: The Definitive Processing Guide and Handbook*, William Andrew Publishing, Norwich, NY, USA (2005).
24. N. Grossiord, P.J.J. Kivit, J. Loos, J. Meuldijk, A.V. Kyrylyuk, P. van der Schoot, and C.E. Koning, *Polymer*, 49, 2866 (2008).
25. M. Sumita, H. Abe, H. Kayaki, and K. Miyasaka, *J. Macromol. Sci. Phys.*, 25, 171 (1986).
26. M.C. Hermant, N.M.B. Smeets, R.C.F. van Hal, J. Meuldijk, J.P.A. Heuts, B. Klumperman, A.M. van Herk and C.E. Koning, *E-Polymers*, 22, 1 (2009).
27. Z. Spitalsky, D. Tasis, K. Papagelis, and C. Galiotis, *Prog. Polym. Sci.*, 35, 357 (2010).
28. J. Tiusanen, D. Vlasveld, J. Vuorinen, and U. Wagenknecht, *Compos. Sci. Technol.*, 72, 1741 (2012).
29. D.H. Morton-Jones, *Polymer Processing*, Chapman and Hall, London (1989).
30. T. Villmow, S. Pegel, P. Pötschke, and U. Wagenknecht, *Compos. Sci. Technol.* 68, 777 (2008).
31. A. Behnam, J. Guo and A.J. Urala, *Appl. Phys.*, 102, 044313 (2007).
32. X.Y. Huang, P.K. Jiang, C. Kim, F. Liu, and Y. Yin, *Eur. Polym. J.*, 45, 377 (2009).
33. S. Bose, A.R. Bhattacharyya, A.P. Bondre, A.R. Kulkarni, and P. Pötschke, *J. Polym. Sci. B: Polym. Phys.*, 46, 1619 (2008).
34. W. Bauhofer and J.Z. Kovacs, *Compos. Sci. Technol.*, 69, 1486 (2009).
35. M. Rahaman, S.P. Thomas, I.A. Hussein, and S.K. De, *Polym. Compos.*, 34, 494 (2013).

36. W. Lu, T.W. Chou, and E.T. Thostenson, *Appl. Phys. Lett.*, 96, 223106 (2010).
37. T. Natsuki, M. Endo, and T. Takahashi, *Phys. A*, 352, 498 (2005).
38. N.A. Bhagat, N.K. Shrivastava, S. Suin, S. Maiti, and B.B.Khatua, *Polym. Compos.*, 34, 787 (2013).
39. K. Levon, A. Margolina, and A.Z. Patashinsky, *Macromolecules*, 26, 4061 (1993).
40. B. Scheibe, E. Borowiak-Palen, and R.J. Kalenczuk, *J. Alloys Compd.*, 500, 117 (2010).
41. K.P. Sau, T.K. Chaki, and D.J. Khastgir, *Appl. Polym. Sci.*, 71, 887 (1999).
42. K.Y. Yan, Q.Z. Xue, Q.B. Zheng, and L.Z. Hao, *Nanotechnology*, 18, 25 (2007).
43. P. Sheng, *Phys. Rev. B.*, 21, 2180 (1980).
44. J.R. Hagerstrom and S.L. Greene, "Electrostatic Dissipating Composites Containing Hyperion Fibril Nanotubes," in *Commercialization of Nanostructured Materials Conference Proceedings*, Miami, Florida, USA, April 6–7 (2000).
45. K. Lozano, J. Bonilla-Rios, and E.V. Barrera, *J. Appl. Polym. Sci.*, 80, 1162 (2001).
46. Y. Ngabonziza, J. Li, and C.F. Barry, *Acta Mech.*, 220(1–4), 289 (2011).
47. J.A. King, B.A. Johnson, M.D. Via, and C.J. Ciarkowski, *J. Appl. Polym. Sci.*, 112(1), 425 (2009).
48. Y.Z. Pan, H.K.F. Cheng, L. Li, S.H. Chan, J.H. Zhao, and Y.K. Juay, *J. Appl. Polym. Sci. B: Polym. Phys.*, 48(21), 2238 (2010).
49. O.A. Moskalyuk, A.N. Aleshin, E.S. Tsobkallo, A.V. Krestinin, and V.E. Yudin, *Phys. Sol. Stabil.*, 54(10), 2122 (2012).
50. K.I. Winey, T. Kashiwagi, and M. Mu, *MRS Bull.* 32, 348 (2007).